ID-1258

MECHANICAL PROPERTIES OF THE Al-25Si-X COMPOSITE AND ITS FRACTURE MECHANISMS

Hyun-Kwang Seok, Jin-Yoo Suh, Ho-In Lee, and Jae-Chul Lee

Div. of Materials Science and Engineering, Korea Institute of Science and Technology
P.O.Box 131, Cheongryang, Seoul, 130-136, Korea (drstone@kist.re.kr)

SUMMARY: If fine Si particles within the hypereutectic Al-Si-X (X is minor elements) alloys are dispersed in the matrix, the alloys can be used as an alternative for the ceramic reinforced composites. The advantages of hypereutectic Al-Si composites over the conventional composites are their superb wear resistance, high modulus, ease of shaping, and low production cost. Such properties make these composites suitable for structural applications, where NVH(Noise vibration harshness) is of significance. To judge the feasibility of the composites for the actual industrial application, we have prepared a propeller shaft using spray-formed Al-Si-X composites, which has been extruded into tubes. In the present study, Young's modulus and mechanical properties of the Al-25Si-X composite were investigated. And then, the fracture mechanisms operative in the hypereutectic Al-Si-X composites were also investigated in an attempt to improve (or tailor) the mechanical properties of the composites suitable for structural applications.

KEYWORDS : Al-Si-X composite, Fracture Mechanism, Mechanical Properties, Structural Applications

INTRODUCTION

Extensive studies on metal matrix composites(MMCs)[1-4] reinforced with ceramic particulates or short fibers have been carried out due to their attractive mechanical properties suitable for structural applications. Although a considerable increase in properties, such as strength, modulus, wear resistance etc., could be achieved by adding ceramic reinforcements, these improvements are always accompanied by a substantial decrease in ductility and enhanced wear rate on opposite parts. In addition, another practical problems in these types of MMCs are relatively high production costs as well as difficulty to machine and recycle.

In recent years, spray-formed hypereutectic Al-Si-X (X is minor elements in wt.%) alloys[5-10], due to their economy of fabrication and ease of mechanical shaping, are gaining a commercial significance for various structural applications that do not require a very high unidirectional strengthening. These composites not only exhibit high strengths equivalent to those of conventional MMCs, but also possess superior wear resistance and high modulus with reasonable ductility. Up to date, most research works on the hypereutectic Al-Si-X composites are focused on wear properties. Several parts such as air compressor rotor[6,7], cylinder liner[7,8], etc., have been commercialized successfully.

An effort to develop hypereutectic Al-Si-X composites suitable for moving(rotating) structural parts, such as propeller shaft for passengers cars, was made recently[13]. Such a component requires materials with high specific modulus to enhance the resonant frequency of the part, thereby reducing noise caused by vibration during service. For safety, the component also requires reasonably high ductility in addition to high strength.

In the present study, Al-25Si-X alloys were fabricated via spray forming and subsequent extrusion. Properties of these composites were altered by varying matrix compositions and heat treatment conditions. Among these samples, two different types of composites (one revealed 0.8% elongation with the tensile strength of 420MPa and the other revealed 16% elongation with 165MPa of the tensile strength) were selected. The fracture mechanisms operative in these composites were investigated by calculating the stress disturbance in the composite.

EXPERIMENTAL PROCEDURES

Al-25Si-X composite preforms were spray formed in rod shapes with dimensions of ϕ300mm x h800mm. The preforms were fabricated with melt temperature of 850-900°C, spray distance of 450mm, substrate withdrawal velocity of 0.2-0.8mm/s at a fixed spray angle of 30°, constant gas pressure of 6 atm, and G/M ratio of 0.8 m^3/Kg[13]. Spray formed rods were then extruded into tubes with the outer diameter and the wall thickness of ϕ120mm x t2mm at 500°C using a 2300 ton capacity hydraulic press[13]. The extruded tubes and their microstructure are shown in Fig.1, where Si particles with average size of ~10 μm are scattered uniformly through out the pore-free matrix.

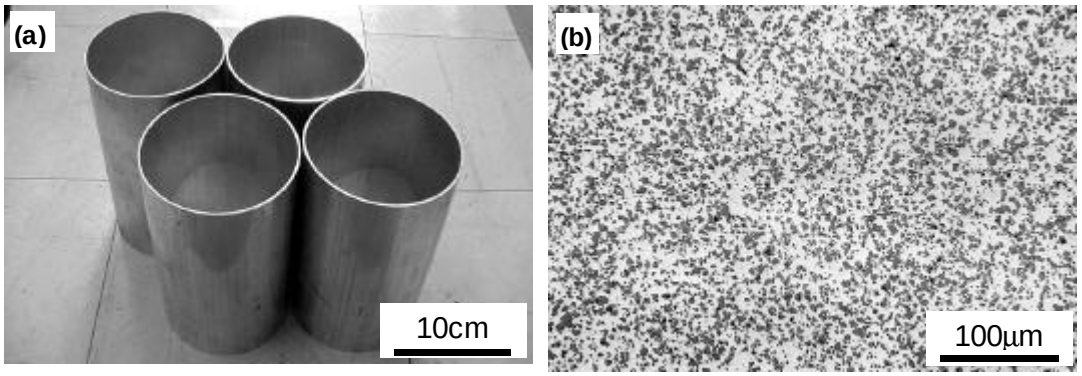

Fig.1 (a) Extruded tubes of spray-formed Al-25Si-X composite and (b) its microstructure.

Prismatic bars were cut out along a direction parallel to extrusion from the extruded tubes to prepare tensile test specimens. Samples were subjected to T4 (495°C for 3 h & quenching) or T6 (T4 & 175°C for 10 h) heat treatments. ASTM tensile test pieces with a rectangular cross-section(w6.25mm) were machined and tested at a room temperature under the constant strain rate of 0.1/min. Fractured specimens were polished in half along a direction parallel to tension mechanically using standard metallographic procedures. The polished surfaces were observed using a scanning electron microscope (SEM) to study the crack initiation and propagation behaviors.

EXPERIMENTAL RESULTS

Mechanical properties of the Al-25Si-X composites

Mechanical properties of the Al-25Si-X composites are listed in Table 1. These experimental results show that the Al-25Si-X composite is suitable for a high Young's modulus material and tailoring of the mechanical properties of the Al-25Si-X composite is possible by designing the composition and heat treatment path.

Table 1. Mechanical properties of the Al-25Si-X composites.

Chemical composition	UTS (MPa)	ε_f (%)	E (GPa)	Heat treatment	Sample #
Al-25Si	164	15.8	89	F	**A**
Al-25Si	166	8.5	89	T4	
Al-25Si-3.67Cu-1.11Mg-0.4Fe	228	2.3	89	F	
Al-25Si-3.67Cu-1.11Mg-0.4Fe	420	0.8	89	T6	**B**

(F: as-fabricated, T4: 495°Cx 3hrs, T6: T4 & 190°Cx10hrs, ε_f : elongation, E : Young's modulus)

Fractographic observations

As shown in Table 1, Elongations of the composites decreased rapidly as the tensile strength increased. Among these composites, two different types of composites, sample **A**(hard/brittle) and sample **B**(soft/ductile) as characterized by tensile properties, were selected and tested under tension to investigate the fracture mechanisms operative in these composites.

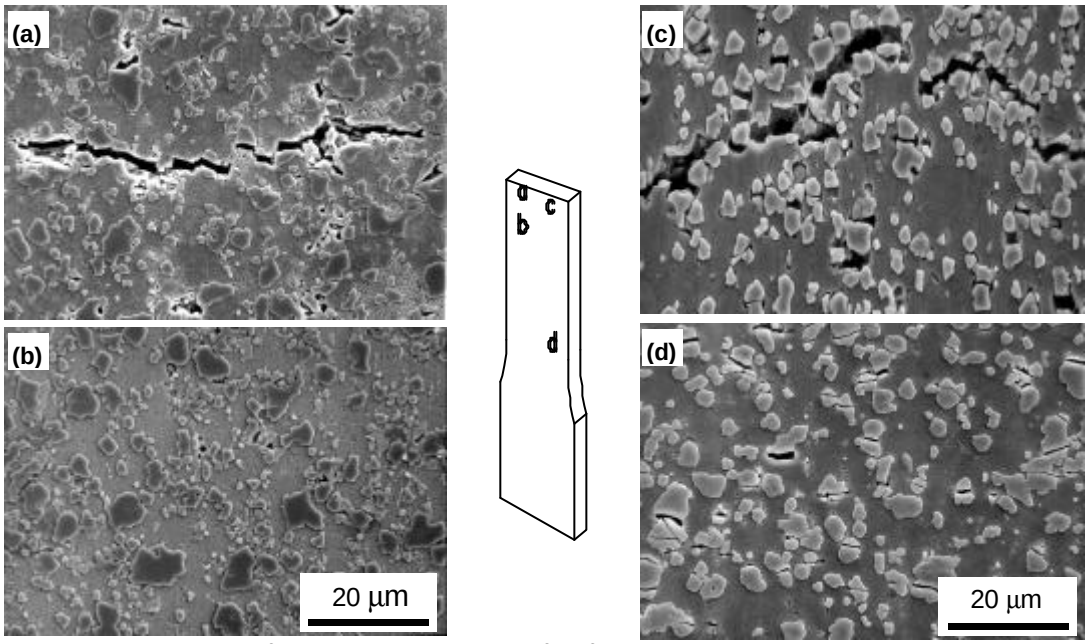

Fig.2 SEM micrographs of the samples observed after fracture test; (a) (b) in sample A, (c), (d) in sample B.

The representative microstructures were recorded from the side surfaces of the fractured samples using SEM. In sample **A**, most Si particles far from the main crack were intact as shown in Fig.2(a) and (b). On the other hand, in sample **B**, which experienced only

about 165MPa of the tensile stress, cracks have been developed uniformly through out the gauge length of the specimen as shown in Fig.2(c) and (d). It is of interest to know the reason why Si particles were fractured at the low tensile strength of 165MPa in sample B.

DISCUSSION

Young's modulus of the composite is sufficiently high for the application of structural material such as vehicle propeller shaft requiring high specific Young's modulus. On the other hand, the tensile properties of the composite should be improved for the usage as the propeller shaft material[13]. Therefore, the fracture mechanisms of the Al-25Si-X composites were investigated by two-dimensional FEM analysis in order to get some informations to improve the tensile properties of the composite.

Model formulation

Considering that most failures are initiated at free surfaces, where the largest stresses develop, actual three-dimensional engineering problems can sometimes be analyzed using a two-dimensional approach. Therefore, a two-dimensional FEM calculation was executed on the domain as in Fig.3, in which 4 rectangular reinforcements are embedded in the matrix. When Al-Si-X composites were extruded, Si particles with large aspect ratios tend to align along a direction parallel to extrusion. Upon loading, cracks can be preferentially initiated in such Si particles and propagate toward the matrix upon increasing the load, so that, the aspect ratio of the reinforcements is assumed as 2[11]. It has been also known that a 90^{o} cleavage plane of the reinforcement to the tensile direction would suffer from the highest tensile stress, and, hence, was the most possible one to be cracked through[12]. However, many experimental results from OM, SEM, and EBSD observations on the Al-25Si-X composites showed that the inner defects such as low angle grain boundary(twin boundary) or cleavage plane do not play an important role in crack development through the Si particles[13]. Therefore, the effects of crystallographic alignment on the fracture procedure is ignored in the FEM calculation.

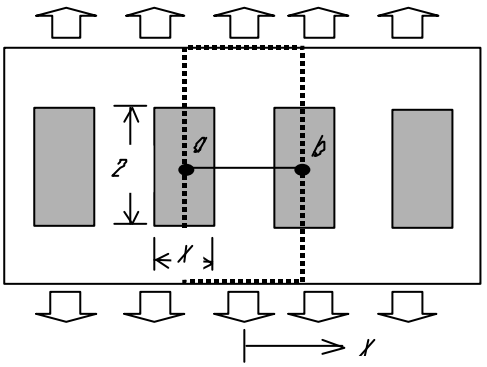

Fig.3 Calculation zone regarded in the FEM analysis of the stress and strain field in Al-25Si-X composite. The aspect ratio and the volume %(=area %) of Si particles are 2 and 25%, respectively.

The volume fraction of the reinforcement within the composite is 25% equal to those of sample A and sample B. The term, d, in Fig.3 denotes the inter-spacing between the

two adjacent Si particles within the calculation zone. Results obtained from the outside of the rectangle denoted by the broken line were not adopted to eliminate the end effect caused by the lateral strain localized at the side surfaces due to the Poisson's ratio. Si particle was regarded as an elastic body having E= 113GPa and ν=0.28, while the matrix was regarded as an elastic-plastic body having E= 70.5GPa and ν=0.34 [14]. The stress-strain data used for FEM analyses were those of sample A and sample B.

Fracture mechanism of the brittle composite

The instant when cracks are initiated in sample **A** is not clear. However, it is thought that cracks were formed just before the eventual fracture of the composite. Such an assumption is reasonable considering that most of Si particles located away from the fracture surface remained intact even after the fracture under 420MPa tensile stress, while Si particles near the main crack were cracked as seen in Fig.2(a) and (b). Assuming that crack is initiated in Si particles under the U.T.S, i.e., 420MPa, in sample **A**, the tensile stress distribution along the line *a* through *b* as marked in Fig.3 was calculated and results are shown in Fig.4(a). As expected, the highest tensile stress more than 500MPa along the tensile axis is concentrated on the edge of Si particles, resulting in the highest possibility for crack initiation at the particle edge. On the contrary, lowest stress is loaded on the matrix near to the interface between particle and matrix. At the instant of crack initiation in Si particle, stress imposed on Si particle should be transferred to matrix resulting in a enormous stress concentration in front of the cracked Si particle as shown in Fig.4(b). Also the tensile stress imposed on the neighbor Si particle in front of the cracked one is increased in a little bit. Therefore, sequential cracks can be developed in another Si particles nearby the previously cracked Si particle due to the load transfer from the neighboring cracked one. When the neighboring particle is cracked, the matrix between two cracked Si particles should fail under ultimately high tensile stress transferred from the both cracked Si particles as shown in Fig.4(c). In this FEM analysis, the effect of plastic deformation zone in front of the crack is ignored to simplify the calculation.

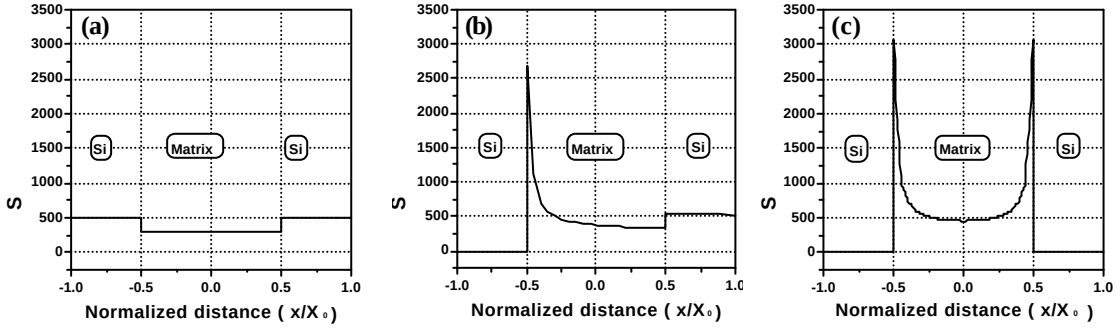

Fig.4 The stress distribution along the line *a* through *b* in Fig.3 when 420MPa stress was loaded on the sample (a) before crack initiation, (b) at the instant of crack initiation in the left-side Si particle, and (c) at the instant of crack development in both Si particles.

Fig.5 shows SEM micrographs focused on the end of the branch of the main crack of the sample A after fracture test, where crack propagates through the matrix and Si particles. In additions, cracked Si particles are observed over the intact matrix in front of the main crack.

These numerical and experimental results say that crack propagates by the sequence of 1) crack initiation in a Si particle, 2) sequential crack development in front of the cracked one, 3) fracture of matrix between the cracked Si particles.

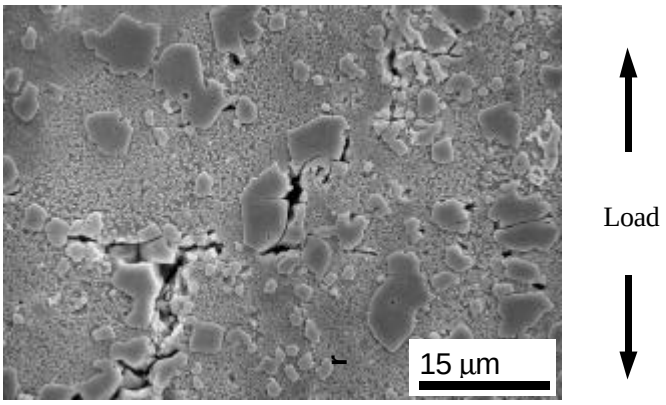

Fig.5 SEM micrograph of the sample A focused on the end of the branch of the main crack.

Fracture mechanism of the ductile composite

In this section, the crack initiation and propagation mechanism of the sample **B** with soft/ductile matrix is discussed.

Fig.6(b) shows the calculation results on the stress distribution in sample **B** calculated on the basis of the measured flow stress curve of sample B as shown in Fig.6(a). As the strain of the sample **B** is increased, the stress concentrated on the reinforcements increased and the inter-spacing between Si particles becomes closer. When the sample is elongated in the range of 7-11%, the maximum stress loaded on the reinforcement is increased up to 485-490MPa, which are almost competitive to the maximum stress loaded on the reinforced Si particles in sample **A** under 420MPa of tensile stress.

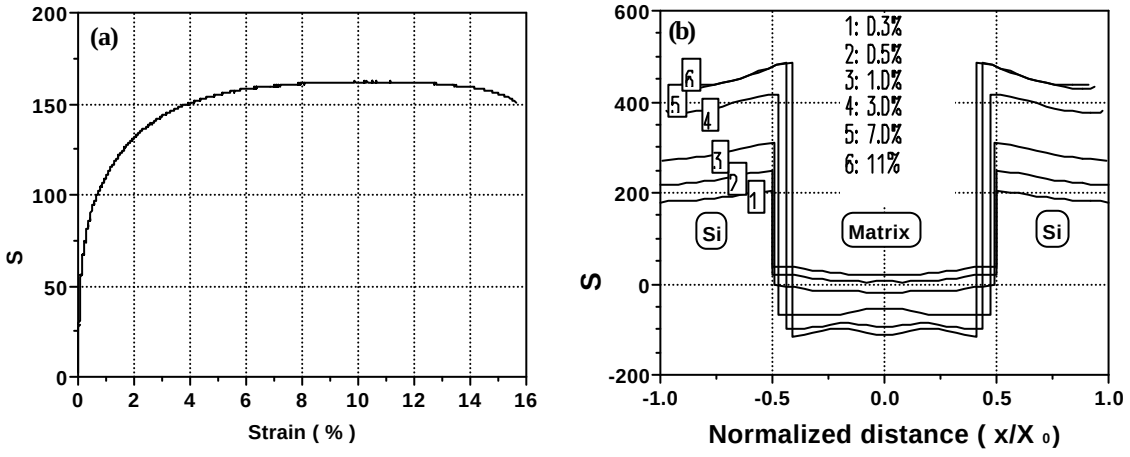

Fig.6 (a) The stress-strain curve of the sample **B**, (b) the variation of stress distribution profiles through the matrix and embedded Si particles with different strain during tensile test.

To determine the critical strain for the crack initiation in sample **B**, tensile test has been interrupted at the elongation of 3%, 5%, 7%, 11%, and 13% and then the microstructure of the test samples have been observed using SEM. The SEM micrographs observed from the

samples elongated in 5%, 7%, and 9% are shown in Fig.7. Few cracked Si particles are observed in the composite elongated to 5% of engineering strain(Fig.7(a)), however, some Si particles are begin to be cracked under 7% elongation(Fig.7(b)). In addition, numerous cracked Si particles are seen when the sample has been elongated up to 9% elongation(Fig.7(c)), resulting in the decrease of engineering stress loaded on the sample as the cracked Si particles do not play the role as reinforcements any more.

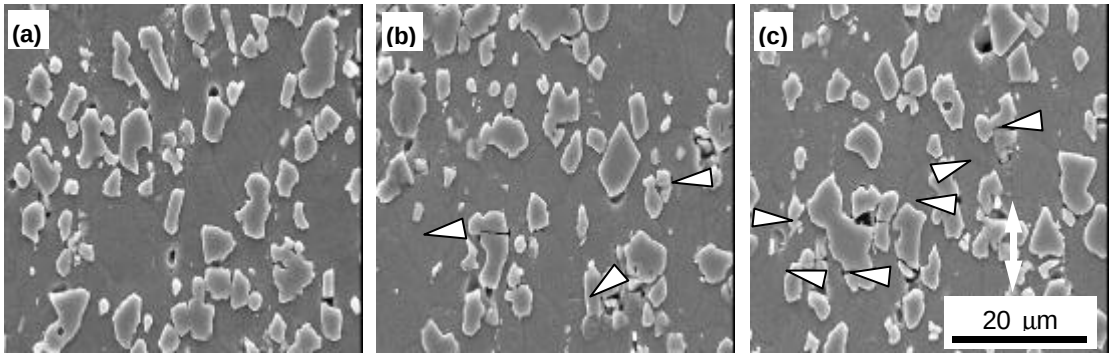

Fig.7 SEM micrographs of the sample B observed after (a) 5% , (b) 7%, and (c) 9% elongation. The arrow indicates the tensile direction.

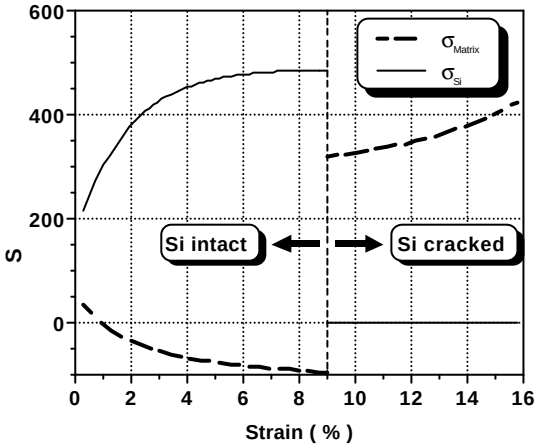

Fig.8 The calculated maximum stress imposed on the matrix and Si particles with increasing strain, where the Si particles are assumed to be cracked under 9% elongation simultaneously.

Fig.8 is the calculation results of the maximum stress imposed on the matrix and Si particles along the line a through b as denoted in Fig.3. It is assumed that the cracks are developed in all Si particles within the calculation zone simultaneously under the 9% of critical strain, where the sample reveals its UTS. Before the critical strain, the stress imposed on the Si particles is increased, on the contrary, the stress imposed on matrix is decreased when the strain is increased. After about 1% elongation, even a compressive stress along the tensile axis is imposed on the matrix because Si particles has a tendency to move to the center of the sample along the lateral direction by tensile stress from remote. At the instant of the crack development under critical strain, the stress imposed on the Si particles should be transferred to the matrix in a flash. As the strain is increased after Si particle cracking, the matrix area, which takes charge of the load, becomes to be decreased, resulting in the increase

of the stress imposed on the matrix. When the stress imposed on the matrix exceeds the fracture stress of the matrix, the matrix between the cracked Si particles could be fractured accompanying local necking, resulting in the eventual fracture of the sample by connection of the cracks developed in Si particles.

Some comments on the model

In the calculation results of Fig.8, the calculated stress imposed on the matrix is overestimated, on the contrary, the stress imposed on Si particles is underestimated. These are because all cracks have been assumed to be developed under 9% elongation but all Si particles are not cracked under the critical strain at the same time in actual tensile test. In addition, Si particles are random-sized and random-dispersed. Therefore, more accurate investigation results can be obtained by regarding the size distribution, cracking time as well as the dispersion position of Si particles. Also, a 3-dimensional model could describe more actual stress condition in the Al-25Si-X composite.

CONCLUSIONS

Two different types of Al-25Si-X composites were prepared by varying matrix composition and heat treatment conditions; the hard/brittle sample(sample **A**) revealed 0.8% elongation with 420MPa U.T.S and the soft/ductile one(sample **B**) revealed 16% elongation with only 165MPa U.T.S. The fracture mechanisms of the samples were investigated via numerical analysis based on FEM calculation and experimental analysis using SEM in order to improve the tensile properties of the composite.

In the case of sample **A**, the cracks developed in Si particles by concentrated stress promote the possibility of another crack development in neighboring Si particles. Therefore, sequential crack can be developed in the Si particle in front of the cracked one preferentially. The matrix between the cracked Si particles should take charge the stress transferred from the Si particles, resulting in fracture of the matrix.

In the case of sample **B**, the stress imposed on the Si particles is increased as the amount of plastic deformation has been increased. When the sample has been elongated to more than 9% strain under the U.T.S. of 165MPa, the stress imposed on the Si particles reached about 490MPa, which are almost competitive to the maximum stress of the reinforcement in elastic-deformed sample **A** under U.T.S of 420MPa. As the cracks in Si particles do not propagate immediately through the soft/ductile matrix after crack development, lots of cracks can be developed in Si particles dispersed all over the test sample even after 9% elongation by high stress imposed on Si particles resulted from sever plastic deformation of the matrix. By increasing the amount of elongation after crack development in lots of Si particles, the matrix between the cracked Si particles would be fractured by accompanying local necking resulting in the eventual fracture of the sample by connecting the cracks developed in Si particles.

ACKNOWLEDGEMENT

Authors really appreciate the help from Dr. Woo-Jin Park with RIST, Korea.

REFERENCES

1. F. Zok, S. Jansson, A.G. Evans, and V. Nardone, "The Mechanical Behavior of a Hybrid Metal Matrix Composite", *Met. Mater. Trans. 22A*, 1991, Vol. 22A , No. 9
2. Keesam Shin, Dongsup Chung, and Sunghak Lee, "The Effect of Consolidation Temperature on Microstructure and Mechanical Properties in Powder Metallurgy", *Met. Mater. Trans. 28A*, 1997, Vol. 28A, No. 12
3. H. Ribes, M. Suery, G. L. L'esperance, and J.G. Legoux, "Microscopic Examination of the Interface Region in 6061-Al/SiC Composites Reinforced with As-received and Oxidized SiC Particles", *Met. Mater. Trans. 21A*, 1990, Vol. 21A, No. 9
4. J.C. Lee, S.B. Park, H.K. Seok, C.S. Oh, and H.I. Lee, "Prediction of Si Contents to Suppress the Interfacial Reaction in the SiCp/2014 Al Composite", *Acta Mater.*, 1998, Vol. 45, No. 8
5. S. P. S. Sangha, D.M. Jacobson, A. J. W. Ogilvy, M. Azema, A. Arun Junai, and E.Botter, " Novel Aluminium-Silicon Alloys for Electronics Packaging", *Materials*, 1997, Vol. 1
6. H. Sano, N. Tokizane, Y. Ohkubo, and K.Sibue, "Spray Formed Aluminium Alloy Components for Automotive Applications", *Powder Metall.*, 1993, Vol. 36, No. 4
7. T. Hayashi, Y. Takeda, K. Akechi, and T. Fujiwara, "Rotary Car Air Conditioner Made with P/M Al-Si Wrought Alloys", *SAE Tech. Paper Series*, 1990, No. 900407
8. M. Scarlett, "Lean Machine", *Engine Technology International*, 1998, Issue 3
9. P.J. Ward, H. V. Atkinson, P.R.G. Anderson, L.G. Elias, B. Garcia, L. Kahlen, and J-M. Rodriguea-Ibabe, "Semi-solid Processing of Novel MMCs Based on Hypereutectic Aluminium-Silicon alloys", *Acta Mater*. 1996, Vol. 44, No. 5
10. H. K. Seok, H.I. Lee, B.J. Kim, and J.C. Lee, "Fabrication of Hypereutectic Al-Si-X Alloy via Spray Forming and Extrusion and Its Feasibility Tests for a Propeller Shaft Application", J. *Kor. Inst. Met. Mater*., 2000, Vol. 38, No. 7
11. J. Llorca, "An Analysis of the Influence of Reinforcement Fracture on the Strength of Discontinuously Reinforced Metal Matrix Composite", *Acta Met. Mater*., 1995, Vol. 43, No. 1
12. N.M. Mawsouf, "A Micromechanical Mechanism of Fracture Initiation in Discontinuously Reinforced Metal-Matrix Composite", *Mater. Charact.*, 2000, Vol. 44
13. H.K. Seok, W.J. Park, H.I. Lee and J.C. Lee, "Fracture Mechanism of the Al-25Si-X Composite Fabricated via Spray Forming and Extrusion 1 - Experimental Investigation", J. Kor. Inst. Met. Mater., 2001, Vol. 39(to be published)
14. E.A. Brandes, G.B. Brook, *Smithells Metalls Reference Book*, 7th Ed., 15-2/15-3